LETTER

doi:10.1038/nature11179

Site-specific DICER and DROSHA RNA products control the DNA-damage response

Sofia Francia[1,2], Flavia Michelini[1], Alka Saxena[3], Dave Tang[3], Michiel de Hoon[3], Viviana Anelli[1]†, Marina Mione[1]†, Piero Carninci[3] & Fabrizio d'Adda di Fagagna[1,4]

Non-coding RNAs (ncRNAs) are involved in an increasingly recognized number of cellular events[1]. Some ncRNAs are processed by DICER and DROSHA RNases to give rise to small double-stranded RNAs involved in RNA interference (RNAi)[2]. The DNA-damage response (DDR) is a signalling pathway that originates from a DNA lesion and arrests cell proliferation[3]. So far, DICER and DROSHA RNA products have not been reported to control DDR activation. Here we show, in human, mouse and zebrafish, that DICER and DROSHA, but not downstream elements of the RNAi pathway, are necessary to activate the DDR upon exogenous DNA damage and oncogene-induced genotoxic stress, as studied by DDR foci formation and by checkpoint assays. DDR foci are sensitive to RNase A treatment, and DICER- and DROSHA-dependent RNA products are required to restore DDR foci in RNase-A-treated cells. Through RNA deep sequencing and the study of DDR activation at a single inducible DNA double-strand break, we demonstrate that DDR foci formation requires site-specific DICER- and DROSHA-dependent small RNAs, named DDRNAs, which act in a MRE11–RAD50–NBS1-complex-dependent manner (MRE11 also known as MRE11A; NBS1 also known as NBN). DDRNAs, either chemically synthesized or *in vitro* generated by DICER cleavage, are sufficient to restore the DDR in RNase-A-treated cells, also in the absence of other cellular RNAs. Our results describe an unanticipated direct role of a novel class of ncRNAs in the control of DDR activation at sites of DNA damage.

Mammalian genomes are pervasively transcribed, with most transcripts apparently not associated with coding functions[4,5]. An increasing number of ncRNAs have been shown to have a variety of relevant cellular functions, often with very low estimated expression levels[6–8]. DICER and DROSHA are two RNase type III enzymes that process ncRNA hairpin structures to generate small double-stranded RNAs[9] (see Supplementary Information).

Detection of a DNA double-strand break (DSB) triggers the kinase activity of ATM, which initiates a signalling cascade by phosphorylating the histone variant H2AX (γH2AX) at the DNA-damage site and recruiting additional DDR factors. This establishes a local self-feeding loop that leads to accumulation of upstream DDR factors in the form of cytologically detectable foci at damaged DNA sites[3,10]. The DDR has been considered to be a signalling cascade made up exclusively of proteins, with no direct contributions from RNA species to its activation.

Oncogene-induced senescence (OIS) is a non-proliferative state characterized by a sustained DDR[11] and senescence-associated heterochromatic foci (SAHF)[12]. Because ncRNAs participate in heterochromatin formation[13], we investigated whether they could control SAHF and OIS. We used small interfering RNAs (siRNAs) to knockdown DICER or DROSHA in OIS cells and monitored SAHF and cell-cycle progression. Knockdown of either DICER or DROSHA, as well as ATM as control[14], restored DNA replication and entry into mitosis (Supplementary Figs 1 and 2); we did not detect overt SAHF changes, however (Supplementary Fig. 3a, b). Instead, we observed that DICER or DROSHA inactivation significantly reduced the number of cells positive for DDR foci containing 53BP1, the autophosphorylated form of ATM (pATM) and the phosphorylated substrates of ATM and ATR (pS/TQ), but not γH2AX, without decreasing the expression of proteins involved in the DDR (Supplementary Fig. 3a–c). Importantly, the simultaneous inactivation of all three GW182-like proteins, TNRC6A, B and C, essential for the translational inhibition mediated by microRNAs (miRNAs; canonical DICER and DROSHA products involved in RNAi)[15], does not affect DDR foci formation (Supplementary Fig. 4).

We next asked whether DICER or DROSHA inactivation also affects ionizing-radiation-induced DDR activation. We transiently inactivated DICER or DROSHA by siRNA in human normal fibroblasts (HNFs), exposed cells to ionizing radiation, and monitored DDR foci. We observed that a few hours after exposure to ionizing radiation, DICER or DROSHA inactivation impairs the formation of pATM, pS/TQ and MDC1, but not γH2AX, foci without decreasing their protein levels (Fig. 1a, b and Supplementary Fig. 5). Furthermore, at an earlier time point (10 min) after ionizing radiation, 53BP1 foci were significantly reduced (Supplementary Fig. 6a). Using an RNAi-resistant form of DICER in DICER knockdown cells, we observed that re-expression of wild-type DICER, but not of a DICER endonuclease mutant (DICER44ab)[16], rescues DDR foci formation (Supplementary Fig. 6b–d). The simultaneous knockdown of TNRC6A, B and C, or DICER has a comparable impact on a reporter system specific for miRNA-dependent translational repression[17], but only DICER inactivation reduces DDR foci formation (Supplementary Fig. 7). To confirm further the involvement of DICER in DDR activation, we used a cell line carrying a hypomorphic allele of *DICER* (*DICER*^{exon5}) defective in miRNA maturation[18]. In *DICER*^{exon5}-irradiated cells, pATM, pS/TQ and MDC1, but not γH2AX, foci formation is impaired without a decrease in their protein levels, and 53BP1 foci formation is delayed compared to the DICER wild-type parental cell line (Supplementary Fig. 8). These defects could be reversed by the re-expression of wild-type DICER but not of the mutant form DICER44ab (Supplementary Fig. 9). By immunoblotting, we confirmed that ATM autophosphorylation is reduced in DICER or DROSHA knockdown HNFs, and in *DICER*^{exon5} cell lines (Supplementary Fig. 10). These results indicate that DICER and DROSHA RNA products control DDR activation and act independently from canonical miRNA-mediated translational repression mechanisms.

DDR signalling enforces cell-cycle arrest at the G1/S and G2/M checkpoints[3]. We observed that DNA-damage-induced checkpoints were impaired in DICER- or DROSHA-inactivated cells and that

[1]IFOM Foundation - FIRC Institute of Molecular Oncology Foundation, Via Adamello 16, 20139 Milan, Italy. [2]Center for Genomic Science of IIT@SEMM, Istituto Italiano di Tecnologia, at the IFOM-IEO Campus, Via Adamello 16, 20139 Milan, Italy. [3]Omics Science Center, RIKEN Yokohama Institute, 1-7-22 Suehiro-cho, Tsurumi-ku, Yokohama, Kanagawa 230-0045, Japan. [4]Istituto di Genetica Molecolare, Consiglio Nazionale delle Ricerche, Pavia 27100, Italy. †Present addresses: Departments of Surgery and Medicine, Weill Cornell Medical College and New York Presbyterian Hospital, 1300 York Avenue, New York, New York 10065, USA (V.A.); Institute of Toxicology and Genetics, Karlsruhe Institute of Technology, 76344 Karlsruhe, Germany (M.M.).

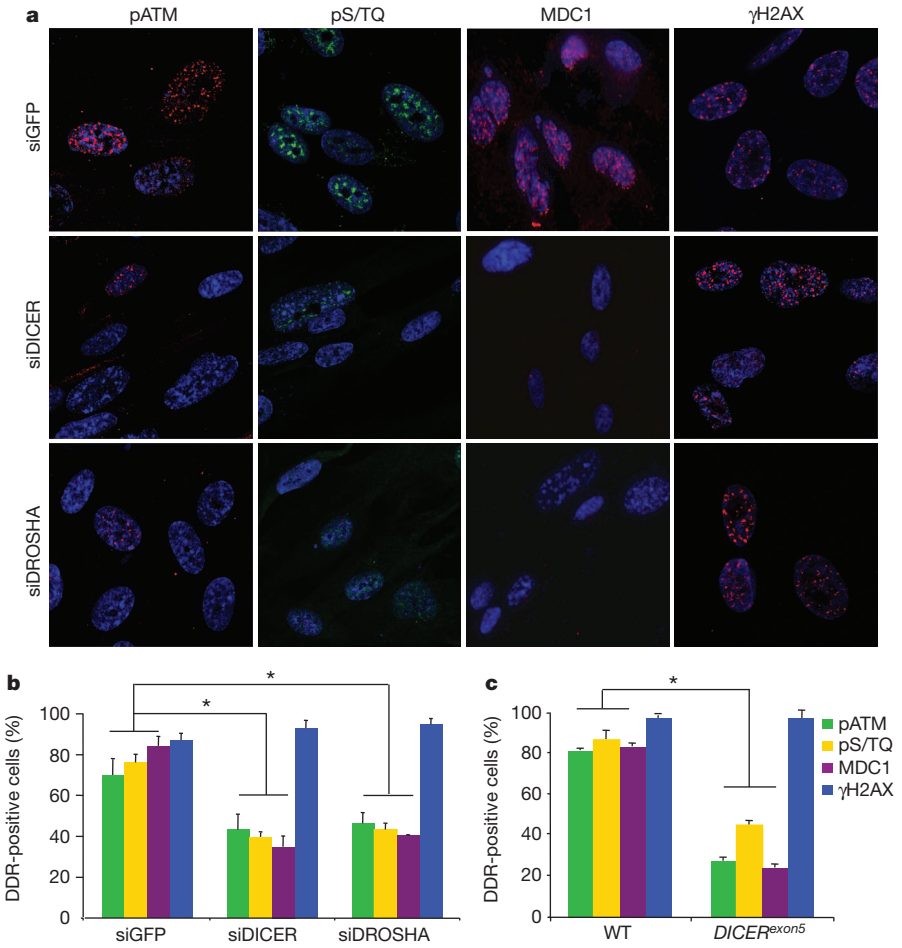

Figure 1 | DICER or DROSHA inactivation impairs DDR foci formation in irradiated cells. **a**, DICER or DROSHA knockdown WI-38 cells were irradiated (10 Gy) and fixed 7 h later. Original magnification, ×250. **b**, Histogram shows the percentage of cells positive for pATM, pS/TQ, MDC1 and γH2AX foci. **c**, Wild-type (WT) and *DICER*^{exon5} cells were irradiated (2 Gy) and fixed 2 h later. Histogram shows the percentage of cells positive for pATM, pS/TQ, MDC1 and γH2AX foci. Error bars indicate s.e.m. ($n \geq 3$). Differences are statistically significant (*P value < 0.01).

wild-type DICER re-expression in *DICER*^{exon5} cells restores checkpoint functions whereas two independent mutant forms of DICER fail to do so (Supplementary Figs 11–13). Thus, DICER and DROSHA are required for DNA-damage-induced checkpoint enforcement.

To test the role of DICER in DDR activation in a living organism, we inactivated it by morpholino antisense oligonucleotide injection in *Danio rerio* (zebrafish) larvae[19]. Such Dicer inactivation results in a marked impairment of pAtm and zebrafish γH2AX accumulation in irradiated larvae as detected both by immunostaining and immunoblotting of untreated or Dicer morpholino-injected larvae and of chimaeric animals (Supplementary Figs 14 and 15).

Previous reports have shown that mammalian cells can withstand transient membrane permeabilization and RNase A treatment, enabling investigation of the contribution of RNA to heterochromatin organization and 53BP1 association to chromatin[20,21]. We used this approach to address the direct contribution of DICER and DROSHA RNA products in DDR activation. Irradiated HeLa cells were permeabilized and treated with RNase A, leading to degradation of all RNAs, without affecting protein levels (Supplementary Fig. 16a). We observed that 53BP1, pATM, pS/TQ and MDC1 foci become markedly reduced in number and intensity upon RNA degradation whereas, similarly to DICER- or DROSHA-inactivated cells, γH2AX is unaffected (Fig. 2a and Supplementary Fig. 16b). Notably, 53BP1, MDC1 and γH2AX triple staining shows that RNA degradation reduces 53BP1 and MDC1 accumulation at unperturbed γH2AX foci (Supplementary Fig. 16c). When RNase A is inhibited, DDR foci progressively reappear within minutes and α-amanitin prevents this (Supplementary Fig. 17a, b), suggesting that DDR foci stability is RNA polymerase II dependent.

We tested whether DDR foci can reform upon addition of exogenous RNA to RNase-A-treated cells. We observed that DDR foci robustly reform in RNase-A-treated cells following their incubation with total RNA purified from the same cells, but not with transfer RNA (tRNA) control (Fig. 2b–d). Similar conclusions were reached using an inducible form of PpoI and AsiSI site-specific endonucleases[22,23] (data not shown).

Next, we attempted to characterize the length of the RNA species involved in DDR foci reformation, which we refer to as DDRNAs. We observed that an RNA fraction enriched by chromatography for species <200 nucleotides was sufficient to restore DDR foci (Supplementary Fig. 17c–e). To attain better size separation, we resolved total RNA on a polyacrylamide gel and recovered RNA fractions of different lengths (Supplementary Fig. 17f, g). Using equal amounts of each fraction, we observed that only the 20–35-nucleotide fraction could restore DDR foci (Fig. 2b), consistent with the size range of DICER and DROSHA RNA products.

To test the hypothesis that DDRNAs are DICER and DROSHA products, we tested DDR foci restoration with total RNA extracted from wild-type or *DICER*^{exon5} cells. Although RNA extracted from wild-type cells restores pATM, pS/TQ and 53BP1 foci, RNA from *DICER*^{exon5} cells does not (Fig. 2c, d). Importantly, RNA from

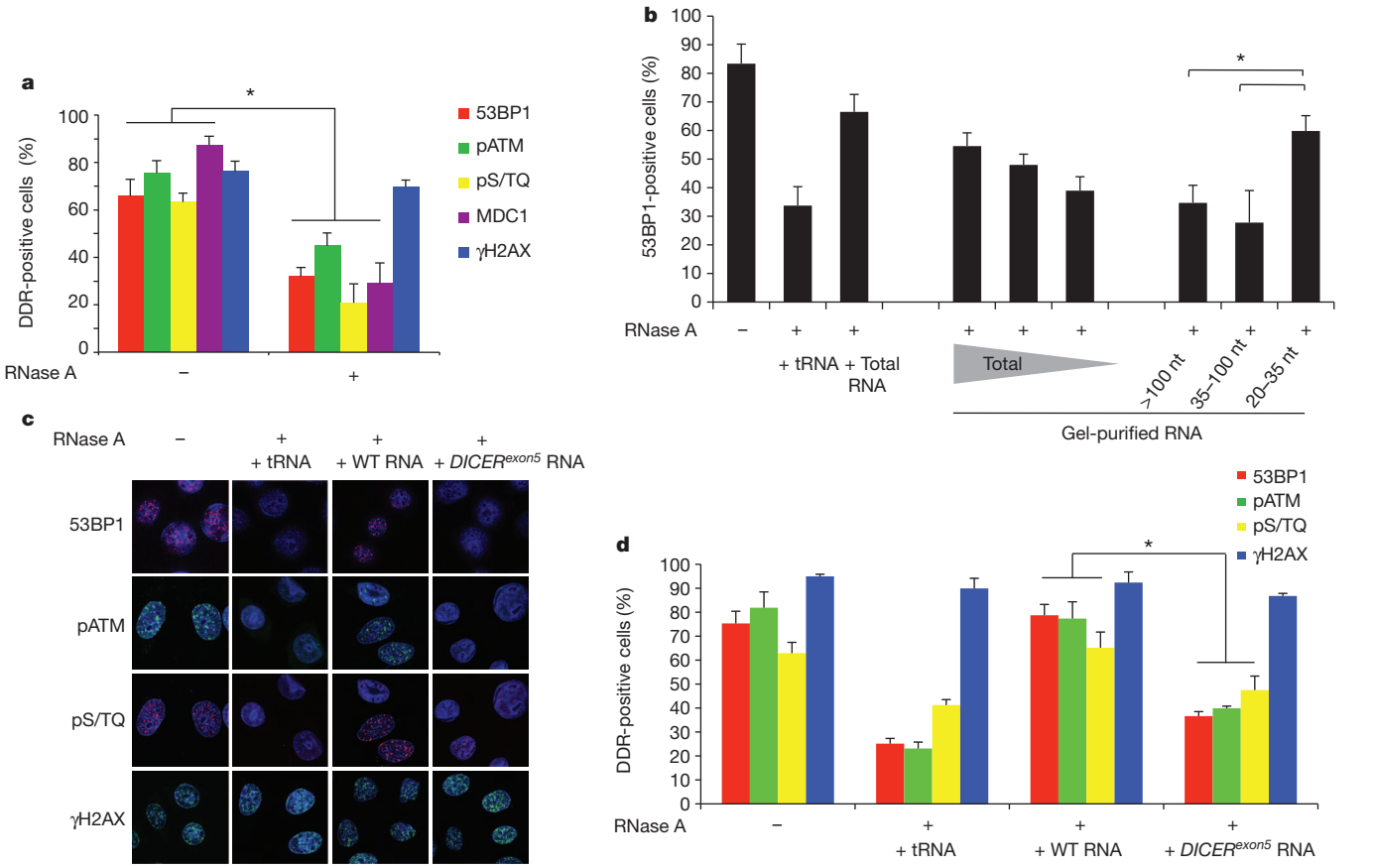

Figure 2 | Irradiation-induced DDR foci are sensitive to RNase A treatment and are restored by small and DICER-dependent RNAs. **a**, Irradiated HeLa cells (2 Gy) were treated with PBS (−) or RNase A (+) and probed for 53BP1, pATM, pS/TQ, MDC1 and γH2AX foci. Histogram shows the percentage of cells positive for DDR foci. **b**, 100, 50 or 20 ng of gel-extracted total RNA and 50 ng of RNA extracted from each gel fraction (>100, 35–100 and 20–35 nucleotides (nt)) were used for DDR foci reconstitution after RNase treatment. **c**, 53BP1, pS/TQ and pATM foci are restored in RNase-treated cells when incubated with RNA of wild-type cells but not with RNA of *DICER*^{exon5} cells or tRNA. Original magnification, ×350. **d**, Histogram shows the percentage of cells positive for DDR foci. Error bars indicate s.e.m. ($n \geq 3$). Differences are statistically significant (*P value < 0.01).

DICER^{exon5} cells re-expressing wild-type, but not endonuclease-mutant, DICER allows DDR foci reformation (Supplementary Fig. 18a, b). These results were reproduced using RNA extracted from cells transiently knocked down for DICER or DROSHA (Supplementary Fig. 18c–f).

Ionizing radiation induces DNA lesions that are heterogeneous in nature and random in their genomic location. To reduce this complexity, we studied a single DSB at a defined and traceable genomic locus. We therefore took advantage of NIH2/4 mouse cells carrying an integrated copy of the I-SceI restriction site flanked by arrays of Lac- or Tet-operator repeats at either sites[24]. In this cell line, the expression of the I-SceI restriction enzyme together with the fluorescent protein Cherry-Lac-repressor allows the visualization of a site-specific DDR focus that overlaps with a focal Cherry-Lac signal (cut NIH2/4 cells). No DDR focus formation is observed overlapping with the Cherry-Lac signal in the absence of I-SceI expression (uncut NIH2/4 cells). Also in this system, RNase A treatment causes the disappearance of the 53BP1, but not the γH2AX, focus at the I-SceI-induced DSB; total RNA addition from cut cells restores 53BP1 focus formation in a dose-dependent manner (Fig. 3a, b). Therefore, a DDR focus generated on a defined DSB can disassemble and reassemble in an RNA-dependent manner.

To determine whether DDRNAs are generated at the damaged locus or elsewhere in the genome, we took advantage of the fact that the I-SceI-induced DSB is generated within an integrated exogenous sequence, which is not present in the parental cell line. As RNAs extracted from NIH2/4 or parental cells are expected to differ only in the potential presence of RNA transcripts generated at the locus, we used these two RNA preparations to attempt to restore 53BP1 focus formation at the I-SceI-induced DSB in RNase-A-treated cells. The formation of the 53BP1 focus was efficiently recovered only by RNA purified from NIH2/4 cells and not from parental cells (Fig. 3c), indicating that DDRNAs originate from the damaged genomic locus.

The MRE11–RAD50–NBS1 (MRN) complex is necessary for ATM activation[25], and pATM and MRE11 foci formation is sensitive to RNase A treatment in the NIH2/4 cell system (Supplementary Fig. 19a, b). To probe the molecular mechanisms by which RNA modulates DDR focus formation, we used a specific MRN inhibitor[26], mirin, which prevents ATM activation also in the NIH2/4 system (Supplementary Fig. 19d). In the presence of mirin, NIH2/4 RNA is unable to restore 53BP1 or pATM focus formation (Fig. 3d, e), indicating that DDRNAs act in a MRN-dependent manner.

To detect potential short RNAs originating from the integrated locus, we deep-sequenced libraries generated from short (<200 nucleotides) nuclear RNAs of cut or uncut NIH2/4 cells, as well as from parental cells expressing I-SceI as negative control. Sequencing revealed short transcripts arising from the exogenous locus (Supplementary Fig. 20a–e), 47 reads in cut cells, 20 reads in uncut cells and none in parental cells, indicating that even an exogenous integrated locus lacking mammalian transcriptional regulatory elements is transcribed and can generate small RNAs.

To test whether the identified locus-specific small RNAs are biologically active and have a causal role in DDR activation, we chemically synthesized four potential pairs among the sequences obtained and used them to attempt to restore the DDR focus in RNase-A-treated

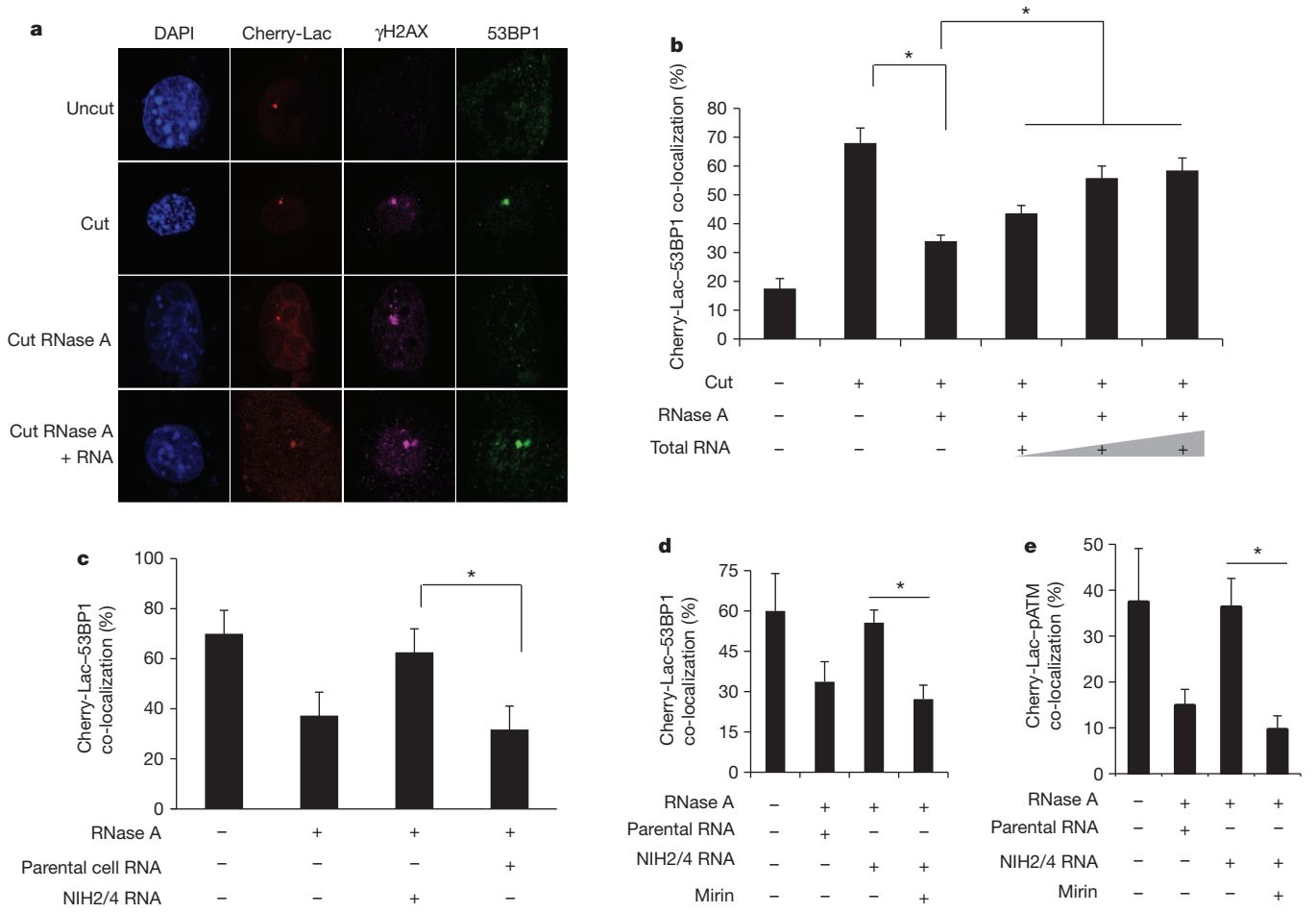

Figure 3 | Site-specific DDR focus formation is RNase A sensitive and can be restored by site-specific RNA in a MRN-dependent manner. a, Cut NIH2/4 cells display a 53BP1 and γH2AX focus co-localizing with a Cherry-Lac focus. 53BP1, but not γH2AX, focus is sensitive to RNase A and is restored by incubation with total RNA. DAPI, 4′,6-diamidino-2-phenylindole. Original magnification, ×450. **b**, Histogram shows the percentage of cells in which 53BP1 and Cherry-Lac foci co-localize. Addition of 50, 200 or 800 ng of RNA purified from cut NIH2/4 rescues 53BP1 foci formation in a dose-dependent manner. **c**, RNA purified from cut NIH2/4 restores 53BP1 focus whereas RNA from parental cells expressing I-SceI does not. **d**, **e**, RNase-A-treated cut NIH2/4 cells were incubated with RNA from cut NIH2/4 cells, or parental ones, to test 53BP1 or pATM focus reformation in the presence of the MRN inhibitor mirin (100 μM). Histogram shows the percentage of cells positive for a DDR focus. Error bars indicate s.e.m. ($n \geq 3$). Differences are statistically significant (*P value < 0.05).

cells. Notably, we observed that addition of locus-specific synthetic RNAs, but not equal amounts of control RNAs, triggers site-specific 53BP1 focus reformation over a large range of concentrations in the presence, but also in the absence, of total RNA from parental cells (Fig. 4a and Supplementary Fig. 20f). To show further the biological activity of RNAs processed by DICER, we *in vitro* transcribed both strands of the sequence spanning the locus, or a control one, and processed the resulting RNAs with recombinant DICER. *In vitro*-generated locus-specific DICER RNA products, but not control RNAs, allowed DDR focus reformation in RNase-A-treated cells even in the absence of parental RNA (Fig. 4b and Supplementary Fig. 20g, h). Overall, these results indicate that DDRNAs are small RNAs with the sequence of the damaged locus, which have a direct role in DDR activation.

To investigate the biogenesis of such RNAs *in vivo*, we performed deeper sequencing of small nuclear RNAs from cut and uncut wild-type as well as DICER or DROSHA knockdown NIH2/4 cells (Supplementary Fig. 21). As expected, DICER or DROSHA knockdown significantly reduced reads mapping to the known miRNAs (Supplementary Fig. 22). Our statistical analyses revealed that the percentage of 22–23-nucleotide RNAs arising from the locus significantly increases in the wild-type cut sample compared to the uncut one and that DICER inactivation significantly reduces it (Supplementary Fig. 23a, b); the detectable decrease in DROSHA-inactivated cells did not reach statistical significance. Because the fraction of 22–23-nucleotide RNAs from the locus is significantly higher with respect to that of non-miRNA genomic loci, the RNAs detected are very unlikely to be random degradation products (Supplementary Fig. 23c). Finally, 22–23-nucleotide RNAs at the locus tend to have an A/U at their 5′ and a G at their 3′ end (Supplementary Fig. 23d), a nucleotide bias significantly different from the originating locus and from the rest of the genome.

In summary, we demonstrate that different sources of DNA damage, including oncogenic stress, ionizing radiation and site-specific endonucleases, activate the DDR in a manner dependent on DDRNAs, which are DICER- and DROSHA-dependent RNA products with the sequence of the damaged site. DDRNAs control DDR foci formation and maintenance, checkpoint enforcement and cellular senescence in cultured human and mouse cells and in different cell types in living zebrafish larvae. They act differently from canonical miRNAs, as inferred by their demonstrated biological activity independent of other RNAs and of GW182-like proteins.

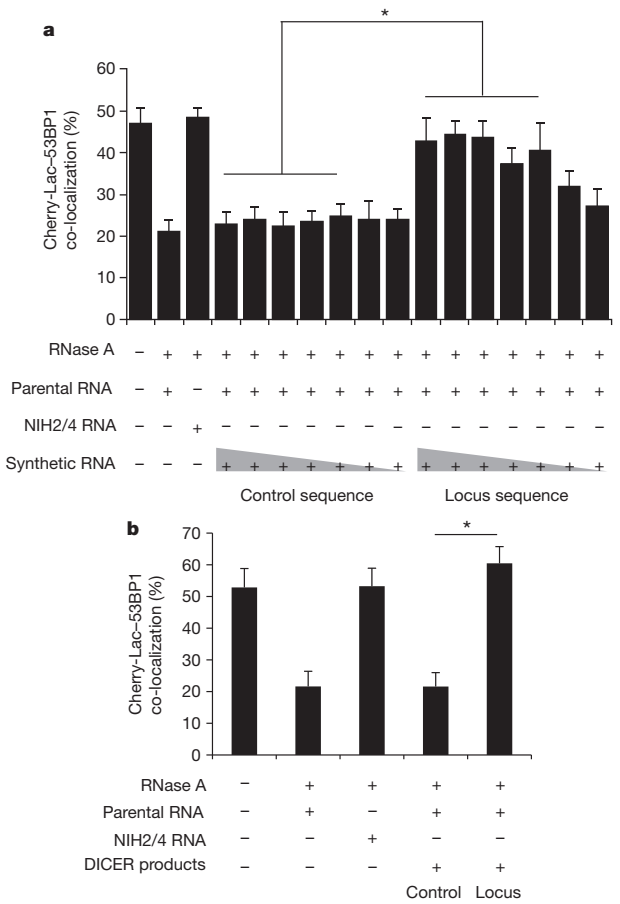

Figure 4 | Chemically synthesized small RNAs and *in vitro*-generated DICER RNA products are sufficient to restore DDR focus formation in RNase-A-treated cells in a sequence-specific manner. a, Chemically synthesized RNA oligonucleotides were annealed and were tested to restore DDR focus formation in RNase-A-treated cut NIH2/4 cells. Mixed with a constant amount (800 ng) of parental cell RNA, a concentration range (1 ng μl^{-1} to 1 fg μl^{-1}, tenfold dilution steps) of locus-specific or GFP RNAs was used. Locus-specific synthetic RNAs (down to 100 fg μl^{-1}) allow site-specific DDR activation. **b**, Small double-stranded RNAs generated by recombinant DICER were tested to restore DDR focus formation in RNase-A-treated cut NIH2/4 cells. 1 ng μl^{-1} RNA was tested mixed with 800 ng of parental cell RNA. Locus-specific DICER RNAs, but not control RNAs, allow site-specific DDR activation. Histograms show the percentage of cells positive for DDR focus. Error bars indicate s.e.m. ($n \geq 3$). Differences are statistically significant (*P value < 0.05).

METHODS SUMMARY

Details of cell cultures, plasmids, siRNAs and antibodies used, as well as descriptions of methods for immunofluorescence, immunoblotting, checkpoint assays, real-time quantitative polymerase chain reaction (PCR), zebrafish injection and transplantation, RNase A treatment, small RNA extraction and purification from gel, RNA sequencing and statistical analyses are provided in Methods.

Full Methods and any associated references are available in the online version of the paper.

Received 8 February 2010; accepted 4 May 2012.
Published online 23 May 2012.

1. Esteller, M. Non-coding RNAs in human disease. *Nature Rev. Genet.* **12,** 861–874 (2011).
2. Krol, J., Loedige, I. & Filipowicz, W. The widespread regulation of microRNA biogenesis, function and decay. *Nature Rev. Genet.* **11,** 597–610 (2010).
3. Jackson, S. P. & Bartek, J. The DNA-damage response in human biology and disease. *Nature* **461,** 1071–1078 (2009).
4. Clark, M. B. *et al.* The reality of pervasive transcription. *PLoS Biol.* **9,** e1000625 (2011).
5. Wilusz, J. E., Sunwoo, H. & Spector, D. L. Long noncoding RNAs: functional surprises from the RNA world. *Genes Dev.* **23,** 1494–1504 (2009).
6. Wang, X. *et al.* Induced ncRNAs allosterically modify RNA-binding proteins *in cis* to inhibit transcription. *Nature* **454,** 126–130 (2008).
7. Zhao, J., Sun, B. K., Erwin, J. A., Song, J. J. & Lee, J. T. Polycomb proteins targeted by a short repeat RNA to the mouse X chromosome. *Science* **322,** 750–756 (2008).
8. Mercer, T. R., Dinger, M. E. & Mattick, J. S. Long non-coding RNAs: insights into functions. *Nature Rev. Genet.* **10,** 155–159 (2009).
9. Kim, V. N., Han, J. & Siomi, M. C. Biogenesis of small RNAs in animals. *Nature Rev. Mol. Cell Biol.* **10,** 126–139 (2009).
10. Lukas, J., Lukas, C. & Bartek, J. More than just a focus: the chromatin response to DNA damage and its role in genome integrity maintenance. *Nature Cell Biol.* **13,** 1161–1169 (2011).
11. d'Adda di Fagagna, F. Living on a break: cellular senescence as a DNA-damage response. *Nature Rev. Cancer* **8,** 512–522 (2008).
12. Narita, M. *et al.* Rb-mediated heterochromatin formation and silencing of E2F target genes during cellular senescence. *Cell* **113,** 703–716 (2003).
13. White, S. A. & Allshire, R. C. RNAi-mediated chromatin silencing in fission yeast. *Curr. Top. Microbiol. Immunol.* **320,** 157–183 (2008).
14. Di Micco, R. *et al.* Oncogene-induced senescence is a DNA damage response triggered by DNA hyper-replication. *Nature* **444,** 638–642 (2006).
15. Tritschler, F., Huntzinger, E. & Izaurralde, E. Role of GW182 proteins and PABPC1 in the miRNA pathway: a sense of deja vu. *Nature Rev. Mol. Cell Biol.* **11,** 379–384 (2010).
16. Zhang, H., Kolb, F. A., Jaskiewicz, L., Westhof, E. & Filipowicz, W. Single processing center models for human Dicer and bacterial RNase III. *Cell* **118,** 57–68 (2004).
17. Nicoli, S. *et al.* MicroRNA-mediated integration of haemodynamics and Vegf signalling during angiogenesis. *Nature* **464,** 1196–1200 (2010).
18. Cummins, J. M. *et al.* The colorectal microRNAome. *Proc. Natl Acad. Sci. USA* **103,** 3687–3692 (2006).
19. Wienholds, E. *et al.* MicroRNA expression in zebrafish embryonic development. *Science* **309,** 310–311 (2005).
20. Maison, C. *et al.* Higher-order structure in pericentric heterochromatin involves a distinct pattern of histone modification and an RNA component. *Nature Genet.* **30,** 329–334 (2002).
21. Pryde, F. *et al.* 53BP1 exchanges slowly at the sites of DNA damage and appears to require RNA for its association with chromatin. *J. Cell Sci.* **118,** 2043–2055 (2005).
22. Berkovich, E., Monnat, R. J. Jr & Kastan, M. B. Roles of ATM and NBS1 in chromatin structure modulation and DNA double-strand break repair. *Nature Cell Biol.* **9,** 683–690 (2007).
23. Iacovoni, J. S. *et al.* High-resolution profiling of γH2AX around DNA double strand breaks in the mammalian genome. *EMBO J.* **29,** 1446–1457 (2010).
24. Soutoglou, E. *et al.* Positional stability of single double-strand breaks in mammalian cells. *Nature Cell Biol.* **9,** 675–682 (2007).
25. Stracker, T. H. & Petrini, J. H. The MRE11 complex: starting from the ends. *Nature Rev. Mol. Cell Biol.* **12,** 90–103 (2011).
26. Dupré, A. *et al.* A forward chemical genetic screen reveals an inhibitor of the Mre11–Rad50–Nbs1 complex. *Nature Chem. Biol.* **4,** 119–125 (2008).

Supplementary Information is linked to the online version of the paper at www.nature.com/nature.

Acknowledgements We thank E. Soutoglou, W. C. Hahn, M. Kastan, V. Orlando, R. Shiekhattar, J. Amatruda, T. Halazonetis, E. Dejana, P. Ng and F. Nicassio for sharing reagents, M. Fumagalli and F. Rossiello for reading the manuscript, M. Dobreva, V. Matti and F. Pezzimenti for technical support, G. D'Ario for help with statistical analyses, B. Amati, M. Foiani, V. Costanzo and F.d.A.d.F. group members for help and discussions. The F.d.A.d.F. laboratory was supported by Fondazione Italiana Ricerca Sul Cancro (FIRC), Associazione Italiana Ricerca sul Cancro (AIRC) European Community's 7th Framework Programme (FP7/2007-2013) under grant agreement no. 202230, acronym "GENINCA", HFSP, AICR, the EMBO Young Investigator Program. The initial part of this project was supported by Telethon grant no. GGP08183. P.C. was supported by 7th Framework of the European Union commission to the Dopaminet consortium, a Grant-in-Aids for Scientific Research (A) no. 20241047, Funding Program for the Next Generation World-Leading Researchers (NEXT Program) to P.C. and a Research Grant to RIKEN Omics Science Center from MEXT. S.F. is supported by Center for Genomic Science of IIT@SEMM (Scuola Europea di Medicina Molecolare) and AIRC. M.M. was supported by Cariplo (grant no. 2007-5500) and AIRC. A.S. is supported by a JSPS fellowship P09745 and grant in aid by JSPS, and D.T. is supported by the European Union 7th Framework Programme under grant agreement FP7-People-ITN-2008-238055 ("BrainTrain" project) to P.C.

Author Contributions A.S., D.T. and P.C. planned, generated and analysed the genomics data presented in Supplementary Figs 20a–e, 21, 22b and 23. M.d.H. performed statistical analysis of the genomics data. A.S. and P.C. also edited the manuscript. M.M. and V.A. generated the data presented in Supplementary Figs 14 and 15. F.M. generated the data shown in Figs 2b, 3d, e, 4b and Supplementary Figs 2b, e, 3e, 4b, 5f, g, 6b–d, 7d, 9, 13d–f, 14d, f, 17f, g, 18a, b, 19, 20g, h and 22a and generated RNA for deep sequencing; contributed to: Supplementary Figs 16a, 5d, e, 11c, d and edited the manuscript. S.F. generated the data shown in remaining figures, contributed to experimental design and edited the manuscript. F.d.A.d.F. conceived the study, designed the experiments and wrote the manuscript.

Author Information Sequence data have been deposited in the DNA Data Bank of Japan under accession code DRA000540. Reprints and permissions information is available at www.nature.com/reprints. The authors declare no competing financial interests. Readers are welcome to comment on the online version of this article at www.nature.com/nature. Correspondence and requests for materials should be addressed to F.d.A.d.F. (fabrizio.dadda@ifom-ieo-campus.it).

METHODS

Cultured cells. Early-passage WI-38 cells (ATCC) were grown under standard tissue culture conditions (37 °C, 5% CO_2) in MEM supplemented with 10% fetal bovine serum, 1% L-glutamine, 1% non-essential aminoacids, 1% Na pyruvate. HeLa, Phoenix ecotrophic and HEK293T cell lines were grown under standard tissue culture conditions (37 °C, 5% CO_2) in DMEM, supplemented with 10% fetal bovine serum, 1% glutamine, 1% penicillin/streptomycin. *DICER*^{exon5} colon cancer cell lines[18] were cultured in McCoy's 5A medium plus 10% fetal calf serum, 1% penicillin/streptomycin. NIH2/4 cells[24] were grown in DMEM, supplemented with 10% fetal bovine serum, 1% glutamine, gentamicine (40 μg ml^{-1}) and hygromycin (400 μg ml^{-1}).

H-RasV12-overexpressing senescent BJ cells were generated as described previously[14]. BrdU incorporation assays were carried out at least 1 week after cultures had fully entered the senescent state, as determined by ceased proliferation, DDR activation and SAHF formation. Ionizing radiation was induced by a high-voltage X-ray generator tube (Faxitron X-Ray Corporation). In general, WI-38 cells were exposed to 5 Gy and transformed cells (RKO, HCT116 and HeLa) to 2 Gy for the DDR foci formation studies. 5 Gy were used for the G2/M checkpoint assays and 10 Gy for the G1/S checkpoint assays.

Cherry-Lac and I-SceI-restriction endonuclease expressing vectors were transfected by lipofectamine 2000 (Invitrogen) in a ratio of 3:1. Sixteen hours after transfection around 70% of the cells were scored positive for DDR markers in the Lac array. For generation of DICER and DROSHA knockdown, NIH2/4 cells were infected with lentiviral particles carrying pLKO.1, shDICER or shDROSHA vectors. After 48 h cells were superinfected with Adeno Empty Vector (gift from E. Dejana) or Adeno I-SceI (gift from P. Ng). Nuclei were isolated the day after the adenoviral infection.

Antibodies. Mouse anti-γH2AX, anti-H3K9me3, rabbit polyclonal anti-pH3 (Upstate Biotechnology); anti-pS/TQ (Cell Signaling Technology); anti-H2AX, anti-H3 and anti-DICER (13D6) (Abcam); rabbit polyclonal anti-53BP1 (Novus Biological); mouse monoclonal anti-53BP1 (gift from T. Halazonetis); anti-MRE11 (gift from S. P. Jackson); anti-BrdU (Becton Dickinson); rabbit polyclonal anti-MCM2 (gift from M. Melixetian); anti-MRE11 rabbit polyclonal raised against recombinant MRE11; anti-pATM (Rockland); mouse monoclonal anti-ATM and anti-MDC1 (SIGMA); anti-Lamin A/C (Santa Cruz); anti-vinculin (clone hVIN-1), anti-β-tubulin (clone AA2) and anti-Flag M2 monoclonal antibodies (Sigma).

Indirect immunofluorescence. Cells were grown on poly-D-lysinated coverslips (poly-D-lysine was used at 50 μg ml^{-1} final concentration) and plated (15–20 × 10^3 cells per cover) 1 day before staining. DDR and BrdU staining was performed as described previously[14]. Cells were fixed in 4% paraformaldehyde or methanol:acetone 1:1. NIH2/4 mouse cells were fixed by 4% paraformaldehyde as described previously[24]. Images were acquired using a wide field Olympus Biosystems Microscope BX71 and the analySIS or the MetaMorph software (Soft Imaging System GmbH). Comparative immunofluorescence analyses were performed in parallel with identical acquisition parameters; at least 100 cells were screened for each antigen. Cells with more than two DDR foci were scored positive. Confocal sections were obtained with a Leica TCS SP2 or AOBS confocal laser microscope by sequential scanning.

Plasmids. DICER–Flag, DICER44ab–Flag and DICER110ab–Flag were a gift from R. Shiekhattar. DICER110ab–Flag and DICER44ab–Flag double mutants carry two amino acid substitutions in the RNase III domains of DICER (Asp 1320 Ala and Asp 1709 Ala for 44ab, and Glu 1652 Ala and Glu 1813 Ala for 110ab mutant; both mutants were reported to be deficient in endonuclease activity[16]). pLKO.1 shDICER-expressing vector was a gift from W. C. Hahn. Short hairpin sequence for DICER is: CCGGCCACACATCTTCAAGACTTAACT CGAGTTAAGTCTTGAAGATGTGTGGTTTTTG. pRETROSUPER shp53 was as described previously[14]. Short hairpin sequence for p53 was: AGTAGATTAC CACTGGAGTCTT. Cherry-Lac-repressor and I-SceI-restriction endonuclease expressing vectors were gifts from E. Soutoglou[24]. shRNA against mouse DICER- and DROSHA-expressing vectors were a gift from W. C. Hahn. shRNA for mouse DICER: CCGGGCCTCACTTGACCTGAAGTATCTCGAGA TACTTCAGGTCAAGTGAGGCTTTTT. shRNA for mouse DROSHA: CCGG CCTGGAATATGTCCACACTTTCTCGAGAAAGTGTGGACATATTCCAGG TTTTTG.

siRNA. The DHARMACON siGENOME SMARTpool siRNA oligonucleotide sequences for human 53BP1, ATM, DICER, DROSHA were as follows. 53BP1: GAGAGCAGAUGAUCCUUUA; GGACAAGUCUCUCAGCUAU; GAUAUC AGC UUAGACAAUU; GGACAGAACCCGCAGAUUU. ATM: GAAUGUU GCUUUCUGAAUU; AGACAGAAUUCCCAAAUAA; UAUAUCACC UGUU UGUUAG; AGGAGGAGCUUGGGCCUUU. DICER: UAAAGUAGCUGGAA UGAUG; GGAAGAGGCUGACUAUGAA; GAAUAUCGAUCCUAUGUUC; GAUCCUAUGUUCAAUCUAA. DROSHA: CAACAUAGACUACACGAUU; CCAACUCCCUCGAGGAUUA; GGCCAACUGUUAUAGAAUA; GAGUAG GCUUCGUGACUUA.

The DHARMACON siGENOME si RNA sequences for human TNRC6A, B and C were as follows. GW182/TNRC6A: GAAAUGCUCUGGUCCGCUA; GCCUAAAUAUUGGUGAUUA. TNRC6B: GCACUGCCCUGAUCCGAUA; GGAAUUAAGUCGUCGUCAU. TNRC6C: CUAUUAACCUCGCCAAUUA; GGUAAGUCCUCCAUUGAUG.

siRNA against human DICER 3′ UTR: CCGUGAAAGUUUAACGUUU. siRNA against GFP: AACACUUGUCACUACUUUCUC. siRNA against luciferase: CAUUCUAUCCUCUAGAGGAUGdTdT; dTdTGUAAGAUAGGAGAUC UCCUAC.

siRNAs were transfected by Oligofectamine or Lipofectamine RNAi Max (Invitrogen) at a final concentration of 200 nM in OIS cells and 100 nM in HNFs. In the siRNA titration experiment OIS cells were transfected in parallel with 20 nM and 200 nM siRNA oligonucleotides. For siRNA transfection with deconvolved siRNA oligonucleotides we used 50 nM for smart pools and 12.5 nM for deconvolved siRNAs.

Real-time quantitative PCR. Total RNA was isolated from cells using TRIzol (Invitrogen) or RNAeasy kit (Qiagen) according to the manufacturer's instructions, and treated with DNase before reverse transcription. For small RNA isolation we used the *mir*Vana miRNA Isolation Kit (Ambion). cDNA was generated using the Superscript II Reverse Transcriptase (Invitrogen) and used as a template in real-time quantitative PCR analysis. TaqMan MicroRNA Assays (Applied Biosystems) were used for the evaluation of mature miR-21 and rnu44 and rnu19 expression levels (assay numbers 000397, 001094 and 001003). 18S or β-actin was used as a control gene for normalization. Real-time quantitative PCR reactions were performed on an Applied Biosystems ABI Prism 7900HT Sequence Detection System or on a Roche LightCycler 480 Sequence Detection System. The reactions were prepared using SyBR Green reaction mix from Roche. Ribosomal protein P0 (RPP0) was used as a human and mouse control gene for normalization.

Primer sequences for real-time quantitative PCR. RPP0: TTCATTGTGGGAG CAGAC (forward), CAGCAGTTTCTCCAGAGC (reverse); human endogenous DICER: AGCAACACAGAGATCTCAAACATT (forward), GCAAAGCAGG GCTTTTCAT (reverse); human endogenous and overexpressed DICER: TGTTCCAGGAAGACCAGGTT (forward), ACTATCCCTCAAACACTCT GGAA (reverse); human DROSHA: GGCCCGAGAGCCTTTTATAG (forward), TGCACACGTCTAACTCTTCCAC (reverse); human GW182: CAGCCAGTCA GAAAGCAGTG (forward), TGTGAGTCCAGGATCTGCTACTT (reverse); mouse DICER: GCAAGGAATGGACTCTGAGC (forward), GGGGACTTCG ATATCCTCTTC (reverse); mouse DROSHA: CGTCTCTAGAAAGGTCCTAC AAGAA (forward), GGCTCAGGAGCAACTGGTAA (reverse).

RNase A treatment and RNA complementation experiments. Cells were plated on poly-D-lysinated coverslips and irradiated with 2 Gy of ionizing radiation. One hour later HeLa cells were permeabilized with 2% Tween 20 in PBS for 10 min at room temperature while I-SceI-transfected NIH2/4 cells were permeabilized in 0.5% Tween 20 in PBS for 10 min at room temperature. RNase A treatment was carried out in 1 ml of 1 mg ml^{-1} ribonuclease A from bovine pancreas (Sigma-Aldrich catalogue no. R5503) in PBS for 25 min at room temperature. After RNase A digestion, samples were washed with PBS, treated with 80 units of RNase inhibitor (RNaseOUT Invitrogen 40 units μl^{-1}) and 20 μg ml^{-1} of α-amanitin (Sigma) for 15 min in a total volume of 70 μl. For experiments with mirin, NIH2/4 cells were incubated at this step also with 100 μM mirin (Sigma) or DMSO for 15 min. Then, RNase-A-treated cells were incubated with total, small or gel-extracted RNA, or the same amount of tRNA, for an additional 15 min at room temperature. If using mirin, NIH2/4 cells were incubated with total RNA in the presence of 100 μM mirin or DMSO for 25 min at room temperature. Cell were then fixed with 4% paraformaldehyde or methanol:acetone 1:1.

In complementation experiments with synthetic RNA oligonucleotides, eight RNA oligonucleotides with the potential to form four pairs were chosen among the sequences that map at the integrated locus in NIH2/4 cells, obtained by deep sequencing. Synthetic RNA oligonucleotides were generated by Sigma with a monophosphate modification at the 5′ end. Sequences map to different regions of the integrated locus: two pairs map to a unique sequence flanking the I-SceI restriction site, one to the Lac-operator and one to the Tet-operator repetitive sequences. Two paired RNA oligonucleotides with the sequences of GFP were used as negative control. Sequences are reported below.

Oligonucleotide 1: 5′-AUAACAAUUUGUGGAAUUCGGCGC-3′, oligonucleotide 2: 5′-CGAAUUCCACAAAUUGUUAUCC-3′, oligonucleotide 3: 5′-AU UUGUGGAAUUCGGCGCCUCUAGAGUCGAGG-3′, oligonucleotide 4: 5′-CC UCGACUCUAGAGGCG-3′, oligonucleotide 5: 5′-AGCGGAUAACAAUUU GUGGCCACAUGUGGA-3′, oligonucleotide 6: 5′-UGUGGCCACAAAUUG UU-3′, oligonucleotide 7: 5′-ACUCCCUAUCAGUGAUAGAGAAAAGUGA

AAGU-3′, oligonucleotide 8: 5′-CUUUCACUUUUCUCUAUCACUGAUAGG GAGUG-3′. GFP 1: 5′-GUUCAGCGUGUCCGGCGAGUU-3′, GFP 2: 5′-CU CGCCGGACACGCUGAACUU-3′.

RNAs were resuspended in 60 mM KCl, 6 mM HEPES, pH 7.5, 0.2 mM $MgCl_2$, at the stock concentration of 12 μM, denatured at 95 °C for 5 min and annealed for 10 min at room temperature.

DICER RNA products were generated as follows. A 550-bp DNA fragment carrying the central portion of the genomic locus studied (three Lac repeats, the I-SceI site and two Tet repeats) was flanked by T7 promoters at both ends and was used as a template for *in vitro* transcription with the TurboScript T7 transcription kit (AMSBIO). The 500-nucleotide-long RNAs obtained were purified and incubated with human recombinant DICER enzyme (AMSBIO) to generate 22–23-nucleotide RNAs. RNA products were purified, quantified and checked on gel. As a control, the same procedure was followed with a 700-bp construct containing the RFP DNA sequence. Equal amounts of DICER RNA products generated in this way were used in a complementation experiment in NIH2/4 cells following RNase A treatment.

Small RNA preparation. Total RNA was isolated from cells using TRIzol (Invitrogen) according to the manufacturer's instructions. To generate small RNA-enriched fraction and small RNA-devoid fraction we used the *mir*Vana microRNA Isolation Kit (Ambion) according to the manufacturer's instructions. The *mir*Vana microRNA isolation kit uses an organic extraction followed by immobilization of RNA on glass-fibre (silica-fibres) filters to purify either total RNA, or RNA enriched for small species. For total RNA extraction ethanol is added to samples, and they are passed through a filter cartridge containing a glass-fibre filter, which immobilizes the RNA. The filter is then washed a few times and the RNA is eluted with a low ionic-strength solution. To isolate RNA that is highly enriched for small RNA species, ethanol is added to bring the samples to 25% ethanol. When this lysate/ethanol mixture is passed through a glass-fibre filter, large RNAs are immobilized, and the small RNA species are collected in the filtrate. The ethanol concentration of the filtrate is then increased to 55%, and it is passed through a second glass-fibre filter where the small RNAs become immobilized. This RNA is washed a few times, and eluted in a low ionic strength solution. Using this approach consisting of two sequential filtrations with different ethanol concentrations, an RNA fraction highly enriched in RNA species ≤200 nucleotides can be obtained[18,27].

RNA extraction from gel. Total RNA samples (15 ng) were heat denatured, loaded and resolved on a 15% denaturing acrylamide gel (1× TBE, 7 M urea, 15% acrylamide (29:1 acryl:bis-acryl)). Gel was run for 1 h at 180 V and stained in GelRed solution. Gel slices were excised according to the RNA molecular weight marker, moved to a 2 ml clean tube, smashed and RNA was eluted in 2 ml of ammonium acetate 0.5 M, EDTA 0.1 M in RNase-free water, rocking overnight at 4 °C. Tubes were then centrifuged 5 min at top speed, the aqueous phase was recovered and RNA was precipitated and resuspended in RNase free water.

G1/S checkpoint assay. WI-38 cells were irradiated with 10 Gy and 1 h afterwards incubated with BrdU (10 μg ml^{-1}) for 7 h; HCT116 cells were irradiated at 2 Gy and incubated with BrdU for 2 h. Cells were fixed with 4% paraformaldehyde and probed for BrdU immunostaining. At least 100 cells per condition were analysed.

G2/M checkpoint assay. HEK 293 calcium phosphate transfected cells were irradiated with 5 Gy and allowed to respond to ionizing-radiation-induced DNA damage in a cell culture incubator for 12, 24 or 36 h. Then, at these three time points after irradiation, together with not irradiated cells, 1×10^6 cells were collected for fluorescence activated cell sorting (FACS) analysis, fixed in 75% ethanol in PBS, 30 min on ice. Afterwards, cells were treated 12 h with 250 μg ml^{-1} of RNase A and incubated for at least 1 h with propidium iodide (PI). FACS profiles were obtained by the analysis of at least 5×10^5 cells. In the complementation experiments HEK 293 cells were transfected using Lipofectamine RNAi Max (Invitrogen) and 48 h later irradiated with 5 Gy. Cells were then treated as explained above.

Immunoblotting. Cells were lysed in sample buffer and 50–100 μg of whole cell lysate were resolved by SDS–PAGE, transferred to nitrocellulose and probed as previously described[14].

For zebrafish immunoblotting protein analysis, 72 h post-fertilization (hpf) larvae were deyolked in Krebs Ringer's solution containing 1 mM EDTA, 3 mM PMSF and protease inhibitor (Roche complete protease inhibitor cocktail). Embryos were then homogenized in SDS sample buffer containing 1 mM EDTA with a pestle, boiled for 5 min and centrifuged at 13,000 r.p.m. for 1 min. Protein concentration was measured with the BCA method (Pierce) and proteins (50—900 μg) were loaded in an SDS-12% (for γH2AX and H3) and SDS-6% polyacrylamide gel (for pATM and ATM), transferred to a nitrocellulose membrane, and incubated with anti-γH2AX (1:2,000, a gift from J. Amatruda[28]), H3 (1:10,000, Abcam), pATM (1:1,000, Rockland), ATM (1:1,000, Sigma). Immunoreactive bands were detected with horseradish-peroxidase-conjugated anti-rabbit or anti-mouse IgG and an ECL detection kit (Pierce). Protein loading was normalized to equal amounts of total ATM and H3.

Zebrafish embryo injection, cell transplantation and staining. Zebrafish embryos at the stage of 1–2 cells were injected with a morpholino against Dicer1[29] diluted in Danieau buffer. The morpholino oligonucleotide was injected at a concentration of 5 ng nl^{-1}, and a volume of 2 nl per embryo. To assess the efficiency of the morpholino to block miRNA maturation, we co-injected the morpholino with *in vitro* synthesized mRNA, encoding for red fluorescent protein (RFP) and carrying three binding sites for miR126 in the 3′ UTR[17]. The oligonucleotides carrying the binding sites for miR126 used for construction of the pCS2:RFPmiR126 sensor are: 5′-GCATTATTACTCACGGTACGAATAAGG CATTATTACTCACGGTACGAATAAGGCATTATTACTCACGGTACGA-3′ and 5′-CGTAATAATGAGTGCCATGCTTATTCCGTAATAATGAGTGCCA TGCTTATTCCGTAATAATGAGTGCCATGCT-3′. The construct was verified by sequencing and used to synthesize mRNA *in vitro* using the mMessage Kit (Ambion). mRNA encoding for RFPmiR126 sensor was injected alone or in combination with Dicer1 morpholino at a concentration of 10 pg nl^{-1}. For cell transplantation experiments, we injected donor embryos with a mixture of *dicer1* morpholino and mRNA encoding for GFP (5 pg nl^{-1}). Approximately 20 cells were transplanted from donor embryos at dome stage (5 hpf) to uninjected host at the same stage. Successfully transplanted larvae (displaying GFP+ cells) were irradiated as described below. Mature miRNAs were reverse transcribed to produce six different cDNAs for TaqMan MicroRNA assay (30 ng of total mRNA for each reaction; Applied Biosystems). Real-time PCR reactions based on TaqMan reagent chemistry were performed in duplicate on ABI PRISM 7900HT Fast Real-Time PCR System (Applied Biosystems). The level of miRNA expression was measured using C_T (threshold cycle). Fold change was calculated as 2^{-CT}.

For immunofluorescence in zebrafish larvae, 72 hpf larvae were irradiated with 12 Gy, fixed in 2% paraformaldehyde for 2 h at room temperature. After equilibration in 10 and 15% sucrose in PBS, larvae were frozen in OCT compound on coverslips on dry ice. Sections were cut with a cryostat at a nominal thickness of 14 μm and collected on Superfrost slides (BDH). Antisera used were zebrafish γH2AX (gift from J. Amatruda[28]) and pATM (Rockland). GFP fluorescence in transplanted embryos was still easily visible in fixed embryos. Images were acquired with a confocal (Leica SP2) microscope and ×63 oil immersion lens.

RNA sequencing. Nuclear RNA shorter than 200 nucleotides was purified using *mir*Vana microRNA Isolation Kit. RNA quality was checked on a small RNA chip (Agilent) before library preparation. For Illumina hi Seq Version3 sequencing, spike RNA was added to each RNA sample in the RNA: spike ratio of 10,000:1 before library preparation and libraries for Illumina GA IIX were prepared without spike. An improved small RNA library preparation protocol was used to prepare libraries[30]. In brief, adenylated 3′ adapters were ligated to 3′ ends of 3′-OH small RNAs using a truncated RNA ligase enzyme followed by 5′ adaptor ligation to 5′-monophosphate ends using RNA ligase enzyme, ensuring specific ligation of non-degraded small RNAs. cDNA was prepared using a primer specific to the 3′ adaptor in the presence of dimer eliminator and amplified for 12–15 PCR cycles using a special forward primer targeting the 5′ adaptor containing additional sequence for sequencing and a reverse primer targeting the 3′ adaptor. The amplified cDNA library was run on a 6% polyacrylamide gel and the 100 bp band containing cDNAs up to 33 nucleotides long was extracted using standard extraction protocols. Libraries were sequenced after quality check on a DNA high sensitivity chip (Agilent). Multiplexed barcode sequencing was performed on Illumina GA-IIX (35 bp single end reads) and Illumina Hi seq version3 (51 bp single end reads).

Statistical analyses. Results are shown as means ± s.e.m. *P* value was calculated by Chi-squared test. Quantitative PCR with reverse transcription results are shown as means of a triplicate ± standard deviation (s.d.) and *P* value was calculated by Student's *t*-test as indicated. *n* stands for number of independent biological experiments.

Statistical analysis of small RNA sequencing data. Statistical significance of downregulation of normalized miRNAs in DICER and DROSHA knockdown samples was calculated using the Wilcoxon signed-rank test.

The differences in the fraction of 22–23 nucleotides versus total small RNAs at the locus between the wild-type, DICER knockdown and DROSHA knockdown before and after cut were calculated by fitting a negative binomial model to the small RNAs count data and performing a likelihood ratio test, keeping the fraction of 22–23-nucleotide versus total small RNAs at the locus fixed across conditions under the null hypothesis and allowing it to vary between conditions under the alternative hypothesis.

27. Duchaine, T. F. *et al.* Functional proteomics reveals the biochemical niche of *C. elegans* DCR-1 in multiple small-RNA-mediated pathways. *Cell* **124,** 343–354 (2006).
28. Sidi, S. *et al.* Chk1 suppresses a caspase-2 apoptotic response to DNA damage that bypasses p53, Bcl-2, and caspase-3. *Cell* **133,** 864–877 (2008).

29. Wienholds, E., Koudijs, M. J., van Eeden, F. J., Cuppen, E. & Plasterk, R. H. The microRNA-producing enzyme Dicer1 is essential for zebrafish development. *Nature Genet.* **35,** 217–218 (2003).

30. Kawano, M. *et al.* Reduction of non-insert sequence reads by dimer eliminator LNA oligonucleotide for small RNA deep sequencing. *Biotechniques* **49,** 751–755 (2010).

Figure supplementary 22

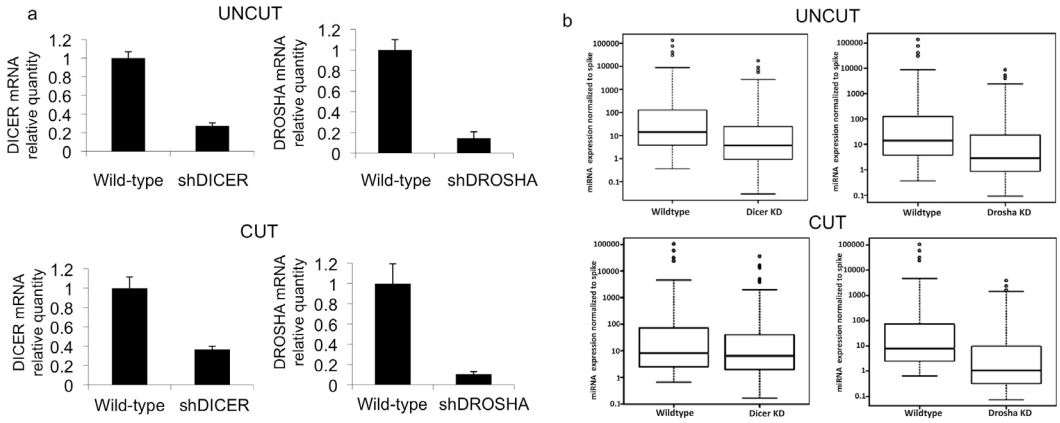

Figure Supplementary 22| DICER and DROSHA knockdown down-regulates miRNAs. a. DICER and DROSHA knockdown by shRNA in uncut and cut samples was evaluated by qRT-PCR. **b.** Reads mapping to the miRNA database miRBase release 18 were normalized with the number of reads of spike in each library. Normalized miRNAs in DICER and DROSHA knockdown samples were compared with wild-type samples before and after cut (as labeled). Statistical significance was calculated using the Wilcoxon signed-rank test. We find that miRNAs are significantly reduced in the DICER and DROSHA knockdown sample compared to the wild-type sample in both cut and uncut conditions (DICER knockdown uncut vs wild-type uncut p =1.544e-263; DROSHA knockdown uncut vs wild-type uncut p =3.843e-279; DICER knockdown cut vs wild-type cut p = 8.911e-84; DROSHA knockdown cut vs wild-type cut p = 1.172e-275).

Figure supplementary 23

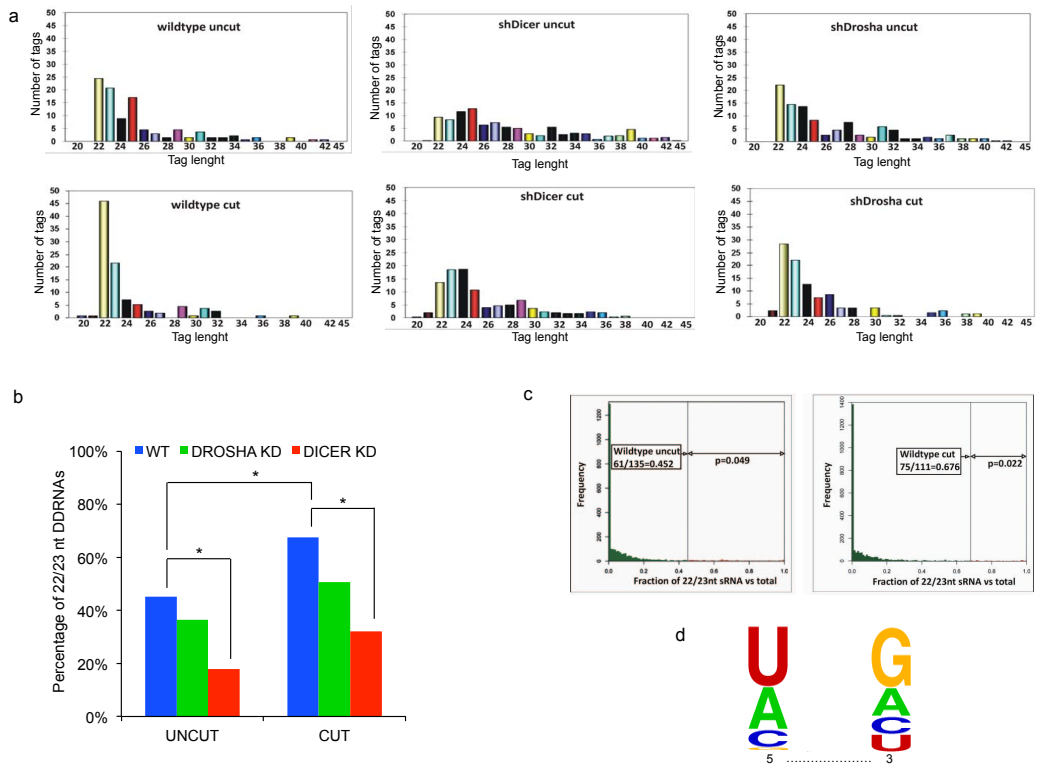

Figure Supplementary 23| Features of short RNAs arising from the locus. a. Length of tags arising from the locus before and after cut. X-axis shows tag lengths in nucleotides and Y-axis depicts number of tags mapping to the locus. The bulk of small RNAs in wild-type samples before and after cut are in the 22-23 nt size range. Among knockdown samples, DICER knockdown shows a broader tag length distribution. **b.** The fraction of 22-23 nt vs total small RNAs at the locus decreases in DICER and DROSHA knockdown samples both in UNCUT and CUT conditions. In DICER knockdown samples, the decrease is statistically significant (in the UNCUT samples p = 4.8e-7, in the CUT samples p=0.029). The fraction of 22-23 nt vs total small RNAs at the locus increases in the wild-type upon cutting (p=0.02). The statistical significance was calculated by fitting a negative binomial model to the small RNA count data and performing a likelihood ratio test, keeping the fraction of 22-23 nt vs total RNAs at the locus fixed across conditions under the null hypothesis and allowing it to vary between conditions under the alternative hypothesis. **c.** The fraction of 22-23 nt reads at the locus is significantly higher than at non miRNA genomic loci. Fractions of 22-23 nt vs total small RNAs at non miRNA genomic loci with at least 50 reads are shown in histograms with the vertical axis depicting their frequency. In each sample, the vertical line depicts the ratio of 22-23 nt RNAs to the total at the locus. The p-value was calculated by summing the area (indicated in red) to the right of this line. We find that the fraction of 22-23 nt vs total small RNAs at the locus studied is significantly higher than the fraction of 22-23 nt tags at non miRNA genomic loci in both uncut (p = 0.049) and cut (p = 0.022) conditions. **d.** The distribution of nucleotides at the 5' and the 3' end of RNA sequences from the locus is significantly different from both the genomic background nucleotide

distribution (p=0.012 at the 5' end and 0.008 at the 3' end) as well as the background nucleotide distribution at the locus (p=0.014 at the 5' end and 1.2e-6 at the 3' end). Specifically, 82.9% sequences start with an A/U and 48.6% sequences end with a G.